2011 American Control Conference
on O'Farrell Street, San Francisco, CA, USA
June 29 - July 01, 2011

Control of an Energy Integrated Solid Oxide Fuel Cell System

Dimitrios Georgis, Sujit S. Jogwar, Ali S. Almansoori† and Prodromos Daoutidis
Department of Chemical Engineering and Materials Science
University of Minnesota, Minneapolis, MN 55455, USA
†Department of Chemical Engineering, The Petroleum Institute, Abu Dhabi, UAE

Abstract— **Solid oxide fuel cell (SOFC) energy systems constitute an alternative solution to the conventional combustion systems for power generation. Their high operating temperature provides the potential for energy integration and higher overall system efficiencies. In this study, an integrated SOFC energy system suitable for stationary applications is considered. Dynamic lumped parameter models for each unit are derived. Control objectives are identified and a control strategy for the integrated SOFC energy system is proposed. A nonlinear model based controller is derived for the control of fuel cell temperature. The effectiveness of the proposed control strategy is illustrated via case studies with varying power demand.**

I. Introduction

Fuel cells provide the most efficient path for the conversion of chemical energy into electrical energy. Recognizing the need for efficient energy production systems and the fact that fuel cells are not limited by Carnot efficiencies, there has been an increasing interest in developing fuel cell systems (see *e.g.* [1], [2] for excellent overviews on recent developments and opportunities in modeling and control of fuel cell systems). Given the challenges associated with the storage and transportation of hydrogen, the *in situ* production of hydrogen from a hydrocarbon fuel, coupled with a hydrogen fuel cell, is a promising approach for power production for stationary fuel cell applications.

SOFCs are high temperature fuel cells with an operating temperature range between $800^oC - 1000^oC$. Besides the fuel flexibility and tolerance to poisoning gases (*e.g.* CO), their high operating temperature is promising for energy integration. The hot effluent streams leaving the SOFC can be recycled through the energy system resulting in improved overall efficiency. Excellent papers are available discussing the basic principles, modeling, dynamics and control of SOFC energy systems (see *e.g.* [3], [4], [5], [6]). SOFC energy integrated configurations have also been proposed along with external [7], [8] as well as internal reforming [8], [9]. The integration of SOFC with gas turbines for increased overall efficiency is another topic of active research (see *e.g.* [10], [11], [12]).

In this paper, we propose an energy integrated configuration (Figure 1) consisting of a solid oxide fuel cell stack, a methane steam reformer, a furnace, a catalytic burner and four heat exchangers used for heat recovery. A similar configuration was studied in [13] (with one less heat recovery loop and without the furnace). Our goal is to demonstrate operational feasibility under meaningful power demand scenarios. To this end, we develop first principle dynamic models for each individual unit. Major control objectives are identified and a control strategy for the entire integrated SOFC energy system is proposed. In order to cope with the nonlinear dynamics associated with the fuel cell, a model based controller is used for the control of the fuel cell stack temperature. The closed-loop performance of the entire energy system is analyzed for varying power demand scenario in the presence of modeling errors.

II. Energy Integrated SOFC System

Figure 1 depicts the proposed energy integrated configuration for the SOFC energy system. Methane, along with steam, is preheated in the heat exchanger HE_1 using the hot effluent stream. The feed stream is further heated in the furnace (F) to the inlet temperature required by the fuel reformer (SR). In the fuel reformer, the steam reforming (strongly endothermic) and water-gas shift (slightly exothermic) reactions take place and a stream rich in hydrogen is produced. This H_2-rich stream is then heated further in the heat exchanger HE_4 before entering the anodic compartment of the SOFC stack. Air is preheated through a series of heat exchangers (HE_2 and HE_3) before entering the cathodic compartment of the SOFC stack. Inside the fuel cell, electrochemical reactions produce both electric power and heat. The SOFC outlet (anodic and cathodic) streams are fed to a catalytic burner (CB) where the unreacted fuels from SOFC (methane, hydrogen and carbon monoxide) are catalytically oxidized to increase the temperature of the effluent stream. The burner's outlet stream is recycled through the heat exchange network in order to provide energy to the fuel and the air streams as well as to the fuel reformer. To improve the controllability of the system, two bypass streams (b_1 and b_2) are added. The first bypass is added across the air heat exchangers while the second bypass is placed across the SOFC cathodic compartment.

A. SOFC Stack

The SOFC stack consists of N single cells connected in series to increase the developed output voltage across an external load. The feed coming into the cathodic and the anodic compartments is equally split into N cells.

Oxygen at the cathode reacts with electrons from the external circuit to form oxide (O^{2-}) ions, which travel across the electrolyte towards the anode. At the anode, hydrogen reacts with the oxide ion to form water, releasing two

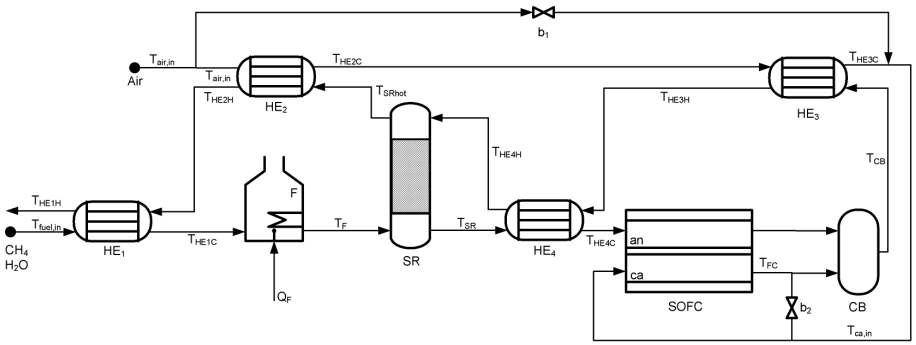

Fig. 1. Basic configuration of the Energy integrated SOFC energy system

electrons. The electrochemical reactions occuring in the fuel cell are the following:

$$\begin{aligned}&\text{Anode: } H_2 + O^{2-} \rightarrow H_2O + 2e^-\\ &\text{Cathode: } \frac{1}{2}O_2 + 2e^- \rightarrow O^{2-}\\ &\Delta H^o_{298} = -241.83 \text{ kJ/mol}\end{aligned}$$

Electric current is produced as a result of the electron flow from the anode to the cathode through an external electric circuit. The open circuit voltage generated by the electrochemical reactions (V_{OCV}) is given by the Nernst equation:

$$V_{OCV} = E_o(T_{FC}) + \frac{RT_{FC}}{2F} ln\left(\frac{p_{H_2}p_{O_2}^{0.5}}{p_{H_2O}}\right) \quad (1)$$

where $E_o(T_{FC})$ represents the standard cell potential (given by $E_o(T_{FC}) = 1.185 - 0.2302 \times 10^{-3}[T_{FC} - T_{ref}]$ [14]) and p_{H_2}, p_{O_2} and p_{H_2O} represent the partial pressures of hydrogen, oxygen and water respectively. However, the actual voltage delivered by the fuel cell is less than the open circuit voltage due to activation (V_{act}), ohmic (V_{ohm}) and concentration (V_{conc}) polarizations. These voltage losses are calculated using the following equations [14]:

$$V_{act} = \frac{RT_{FC}}{F} sinh^{-1}\left(\frac{I}{2I_o}\right) \quad (2)$$

$$V_{ohm} = I \times R_i \quad (3)$$

$$V_{conc} = \frac{RT}{2F} ln\left(\frac{I_L}{I_L - I}\right) \quad (4)$$

where I is the electric current, I_o is the apparent exchange current, R_i is the internal resistance of the cell (temperature dependent) and I_L is the limited current. The voltage and power the SOFC stack delivers to a load is then given by:

$$V = N\left(V_{OCV} - V_{act} - V_{ohm} - V_{conc}\right) \quad (5)$$

$$P = V \times I \quad (6)$$

Recent studies (*e.g.* [15]) have shown, through experimental validation, that lumped parameter models of SOFC systems provide sufficient accuracy for systems level analysis and control design purposes. Motivated by this we derive lumped parameter models for both the species and energy balances. We assume constant pressure, ideal gas behavior and adiabatic operation of the fuel cell. The species and energy balances take then the following form:

$$\begin{aligned}\frac{dn_{FC,H_2}}{dt} &= \dot{n}_{FC,H_2,in} - \dot{n}_{FC,H_2} - \frac{I}{2F}\\ \frac{dn_{FC,H_2O}}{dt} &= \dot{n}_{FC,H_2O,in} - \dot{n}_{FC,H_2O} + \frac{I}{2F}\\ \frac{dn_{FC,O_2}}{dt} &= \dot{n}_{FC,O_2,in} - \dot{n}_{FC,O_2} - \frac{I}{4F}\\ \frac{dT_{FC}}{dt} &= \frac{1}{\rho_c C_{p,c} V_c}\Big[\dot{Q}_{an,in} + \dot{Q}_{ca,in} - \dot{Q}_{an,out} -\\ &\dot{Q}_{ca,out} - \Delta H_e \frac{I}{2F} - \frac{VI}{N}\Big]\end{aligned} \quad (7)$$

where the subscripts an and ca refer to the anode and cathode properties, ΔH_e is the heat of the electrochemical reaction and $\dot{Q}$ represents the enthalpy flow, calculated as:

$$\dot{Q}(T) = \sum_i \dot{n}_i \int_{T_{ref}}^{T} C_{p,i}(\tilde{T}) d\tilde{T} \quad (8)$$

At the cathode, the outlet total flow rate, $\dot{n}_{ca,out}$, is given by:

$$\dot{n}_{ca,out} = \dot{n}_{ca,in} - I/4F \quad (9)$$

where $I/4F$ represents the rate of oxygen consumption inside the SOFC.

B. Steam Reformer

Preheated methane and steam enter the steam reformer where the following two reactions take place:

$$\begin{aligned}CH_4 + H_2O \rightleftharpoons CO + 3H_2 \quad \Delta H^o_{298} = +206.1 \text{ kJ/mol}\\ CO + H_2O \rightleftharpoons CO_2 + H_2 \quad \Delta H^o_{298} = -41.15 \text{ kJ/mol}\end{aligned}$$

The first (steam reforming) reaction is highly endothermic while the second (water-gas shift) reaction is slightly exothermic. However, the overall reaction is highly endothermic, thus requiring continuous energy input to keep the hydrogen production at high levels. The required energy is provided by the hot effluent stream coming out from HE_4 (see Figure 1).

Here, we assume constant pressure and ideal gas behavior. Thus the species balance equations are expressed by the following equations:

$$
\begin{aligned}
\frac{dn_{SR,CH_4}}{dt} &= \dot{n}_{SR,CH_4,in} - \dot{n}_{SR,CH_4} - m_{cat}\cdot r_1 \\
\frac{dn_{SR,H_2O}}{dt} &= \dot{n}_{SR,H_2O,in} - \dot{n}_{SR,H_2O} - m_{cat}\cdot (r_1 + r_2) \\
\frac{dn_{SR,CO_2}}{dt} &= \dot{n}_{SR,CO_2,in} - \dot{n}_{SR,CO_2} + m_{cat}\cdot r_2 \\
\frac{dn_{SR,CO}}{dt} &= \dot{n}_{SR,CO,in} - \dot{n}_{SR,CO} + m_{cat}\cdot (r_1 - r_2) \\
\frac{dn_{SR,H_2}}{dt} &= \dot{n}_{SR,H_2,in} - \dot{n}_{SR,H_2} + m_{cat}\cdot (3r_1 + r_2)
\end{aligned} \tag{10}
$$

where r_1 and r_2 refer to the rates of the steam reforming and the water-gas shift reaction respectively [16]. The energy balance equations take the form:

$$
\begin{aligned}
\frac{dT_{SR}}{dt} &= \frac{1}{\varepsilon\rho_g(T_{SR})C_{p,g}(T_{SR}) + (1-\varepsilon)\rho_{cat}C_{p,cat}} \times \\
&\quad \Big(\dot{Q}_{fuel,in} - \dot{Q}_{fuel,out} + UA_{SR}\Delta T_{LM} \\
&\quad -m_{cat}\left(r_1\Delta H_1 + r_2\Delta H_2\right)\Big) \\
\frac{dT_{SR_{hot}}}{dt} &= \frac{1}{MC_p(T_{SR_{hot}})}\Big(\dot{Q}_{hot,in} - \dot{Q}_{hot,out} \\
&\quad -UA_{SR}\Delta T_{LM}\Big)
\end{aligned} \tag{11}
$$

where MC_p refers to the fluid's heat capacity, ε represents the void fraction of the catalytic bed and ΔT_{LM} is the log mean temperature difference.

C. Catalytic Burner

The streams coming from the fuel cell are fed to the catalytic burner where complete combustion of methane, hydrogen and carbon monoxide is assumed to occur. The air required for complete combustion is provided by the SOFC (note that excess air is provided in the SOFC). Additional air may be added if needed. The temperature dynamics for the catalytic burner is described with the following equation:

$$
\frac{dT_{CB}}{dt} = \frac{1}{MC_p(T_{CB})}\left(\dot{Q}_{in} - \dot{Q}_{out} - \sum_{i=3}^{5}\dot{n}_i^r\Delta H_i\right) \tag{12}
$$

where $\dot{n}_3^r$, $\dot{n}_4^r$, $\dot{n}_5^r$ refer to the reacted moles of methane, hydrogen and carbon monoxide while ΔH_3, ΔH_4 and ΔH_5 represent the corresponding heats of combustion.

D. Furnace

The furnace provides the extra energy required to increase the methane/steam stream temperature. Its energy dynamics are described by the following equation:

$$
\frac{dT_F}{dt} = \frac{1}{MC_p(T_F)}\left(\dot{Q}_{F,in} - \dot{Q}_{F,out} + \dot{Q}_F\right) \tag{13}
$$

where $\dot{Q}_F$ is the furnace heat duty.

E. Heat Exchangers

Process heat exchangers are placed in order to recover the energy coming from the hot effluent stream. Their energy dynamics are captured by the following equations:

$$
\begin{aligned}
\frac{dT_{HEi_C}}{dt} &= \frac{1}{MC_p(T_{HEi_C})}\Big(\dot{Q}_{HEi_C,in} \\
&\quad -\dot{Q}_{HEi_C,out} + UA_{HEi}\Delta T_{LM}\Big) \\
\frac{dT_{HEi_H}}{dt} &= \frac{1}{MC_p(T_{HEi_H})}\Big(\dot{Q}_{HEi_H,in} \\
&\quad -\dot{Q}_{HEi_H,out} - UA_{HEi}\Delta T_{LM}\Big)
\end{aligned} \tag{14}
$$

where i denotes to the heat exchanger number and the H and C subscripts refer to the hot and cold streams respectively.

III. Control of The SOFC Energy System

The control objectives considered for the entire integrated system are the following:

- *Fuel cell temperature control*: Fuel cell temperature should be maintained under a maximum value to avoid the development of thermal stresses which can damage the cell components. In addition, fuel cell temperature should be maintained at high levels to ensure high ionic conductivity of the electrolyte.
- *Fuel Utilization (U_F) control*: Fuel utilization (the ratio of the reacted hydrogen flow rate over the inlet hydrogen flow rate) should be controlled in order to prevent any fuel starvation conditions at the anode. Fuel starvation conditions can cause serious damage to the anode.
- *Reformer inlet temperature control*: In order to ensure steady hydrogen production, the reformer inlet temperature should be kept constant.
- *Fuel cell air inlet temperature*: The air inlet temperature needs to be regulated at a specific level in order to avoid large temperature gradients along the fuel cell.
- *Fuel cell power control*: The SOFC energy system should be a feasible and reliable power supply system under frequent variations in the power demand.

A. Fuel cell temperature control

The fuel cell temperature represents a key variable in the operation of the energy system. Given the highly nonlinear nature of the fuel cell model presented in the previous section, it is meaningful to implement a model based controller to maintain the fuel cell temperature at the desired value. To this end, we derived a nonlinear output feedback linearizing controller using the bypass ratio (b_2) as manipulated input. The controller was based on a combination of state feedback and an open-loop observer (see [18] for details), and incorporates the load current measurement. The relative degree between the input and the output is 1, so a response of the form:

$$
\beta\frac{dT_{FC}}{dt} + T_{FC} = \upsilon \tag{15}
$$

was requested. The auxiliary input υ is given by a simple PI controller of the form:

$$
\begin{aligned}
\upsilon &= T_{FC,sp} + T_{FC,sp} * K_{FC} \times \\
&\quad \left((T_{FC,sp} - T_{FC}) + \frac{1}{\tau_{I,FC}}\int_0^t (T_{FC,sp} - T_{FC})d\tilde{t}\right)
\end{aligned} \tag{16}
$$

where the subscript sp denotes the set point.

B. Fuel cell power control

Power control is achieved at the electrical side of the fuel cell system through the use of power electronics. Specifically, a buck-boost DC/DC converter is placed after the SOFC which can either increase or decrease the output voltage at constant power. More sophisticated control structures are available [19], however, our interest is focused more on the chemical side hence a simplified control structure is used for the power control.

The control of the power production level through the DC/DC converter is achieved by implementing a cascade of two PI controllers (see Figure 2) [17]. The power controller

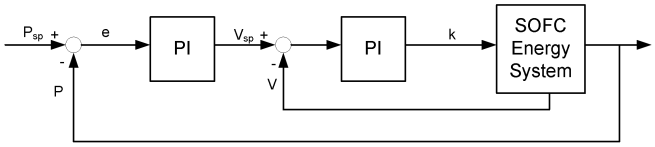

Fig. 2. Power Control Structure

(outer loop) generates the set point for the voltage controller (internal loop). The power control law takes the following form:

$$V_{sp} = V_{nom} + K_P \left((P_{sp} - P) + \frac{1}{\tau_{I,P}} \int_0^t (P_{sp} - P) d\hat{\tau} \right) \quad (17)$$

where the subscript nom represents the nominal value of the parameter. Afterwards, the voltage controller controls the voltage at the new desired level by manipulating the gain of the DC/DC converter's switch. The voltage control law is expressed by the following equation:

$$k = k_{nom} + K_V \left((V_{sp} - V) + \frac{1}{\tau_{I,V}} \int_0^t (V_{sp} - V) d\hat{\tau} \right) \quad (18)$$

C. Fuel Utilization (U_F) control

The use of the electrical side for the control of fuel cell power leads to sub-efficient fuel utilization. The fuel utilization control can be achieved through the manipulation of the fuel flow into the system. A PI controller is used to achieve this objective:

$$\begin{aligned} \dot{n}_{fuel} &= \dot{n}_{fuel,nom} + K_{U_F} \left((U_{F,sp} - U_F) + \right. \\ &\left. \frac{1}{\tau_{I,U_F}} \int_0^t (U_{F,sp} - U_F) d\tilde{t} \right) \end{aligned} \quad (19)$$

D. Reformer inlet temperature control

The natural choice for manipulated input for this control loop is the furnace duty ($\dot{Q}_F$). A PI controller of the form:

$$\begin{aligned} \dot{Q}_F &= \dot{Q}_{F,nom} + K_F \left((T_{F,sp} - T_F) + \right. \\ &\left. \frac{1}{\tau_{I,T_F}} \int_0^t (T_{F,sp} - T_F) d\tilde{t} \right) \end{aligned} \quad (20)$$

is used to achieve this control objective.

E. Fuel cell air inlet temperature

The fuel cell air inlet temperature is controlled by manipulating the bypass ratio b_1. A PI controller is used for the control of this variable:

$$\begin{aligned} b_1 &= b_{1,nom} + K_{T_{ca,in}} \left((T_{ca,in,sp} - T_{ca,in}) + \right. \\ &\left. \frac{1}{\tau_{I,T_{ca,in}}} \int_0^t (T_{ca,in,sp} - T_{ca,in}) d\hat{\tau} \right) \end{aligned} \quad (21)$$

Table II contains all the controller parameters that have been used.

IV. Simulation results

First, the performance of the nonlinear temperature controller was compared with that under PI controller (with the same K_{FC} and $\tau_{I,FC}$ as in Eq. (16)). Figure 3 shows the corresponding response of the system for an increase in the power demand from 16.4 kW to 17.0 kW. It can be noted that the nonlinear controllers works much better compared to the linear controllers. Also, the nonlinear controller is quite robust to modeling errors. As seen from Figure 3, an error of 5% in modeling the heat of reaction in the fuel cell maintains superior performance over its linear counterpart.

Next, a varying power demand scenario was considered, where steps in the power demand were applied hourly. Table I shows the parameters corresponding to the nominal operating point. We apply an increase in the power demand to 17 kW, then decrease the power demand to 15 kW with a step rate change of 0.5 kW/hr and then increase it again to 16.6 kW. Figures 4 to 9 show the closed loop responses of the controlled variables along with their manipulated variables. The proposed control strategy performs well in achieving the requested power demand, while maintaining the other control variables at their nominal values.

V. Conclusions

In this paper, we proposed an energy integrated SOFC configuration consisting of a SOFC stack, a fuel reformer, a catalytic burner, a furnace and heat exchangers. First principle dynamic models were derived for each unit. A control strategy for the entire SOFC energy system was developed. A control system comprising of a nonlinear feedback-feedforward controller for fuel cell temperature, a cascade controller for power control and three proportional integral controllers is implemented. The nonlinear fuel cell temperature controller was compared with a linear controller.

TABLE I

NOMINAL PARAMETERS FOR THE SOFC ENERGY SYSTEM

N	384	$T_{ca,in}$	973.1 K
V	272.1 V	T_{CB}	1312.1 K
I_L	60.3 A	T_F	822.9 K
R_L	4.5 Ω	T_{SR}	932.3 K
P	16.4 kW	$T_{SR,hot}$	934.8 K
U_F	0.8	T_{HE1C}	668.5 K
T_{FC}	1153 K	T_{HE1H}	518.1 K
P_{FC}	1.01 bar	T_{HE2C}	673.9 K
Q_F	1.7 kW	T_{HE2H}	678.6 K
b_1	0.10	T_{HE3C}	1048.1 K
b_2	0.10	T_{HE3H}	1064.0 K
$\dot{n}_{fuel}$	0.225 mol/s	T_{HE4C}	973.4 K
$\dot{n}_{air}$	1.754 mol/s	T_{HE4H}	1057.6 K
S/C	4	x_{CH_4}	0.926

TABLE II

CONTROLLER PARAMETERS FOR BOTH THE CONTROL SYSTEMS

β (min)	5
K_P (VW^{-1})	0.5
$\tau_{I,P}$ (s)	10
K_V (V^{-1})	$1 \cdot 10^{-4}$
$\tau_{I,V}$ (s)	1
$K_{T_{FC}}$ (K^{-1})	$5 \cdot 10^{-3}$
$\tau_{I,T_{FC}}$ (s)	250
K_{T_F} (WK^{-1})	2
τ_{I,T_F} (s)	70
K_{U_F} (s/mol)	$2 \cdot 10^{-2}$
τ_{I,U_F} (s)	20
$K_{T_{ca,in}}$ (K^{-1})	$1 \cdot 10^{-3}$
$\tau_{I,ca,in}$ (s)	50

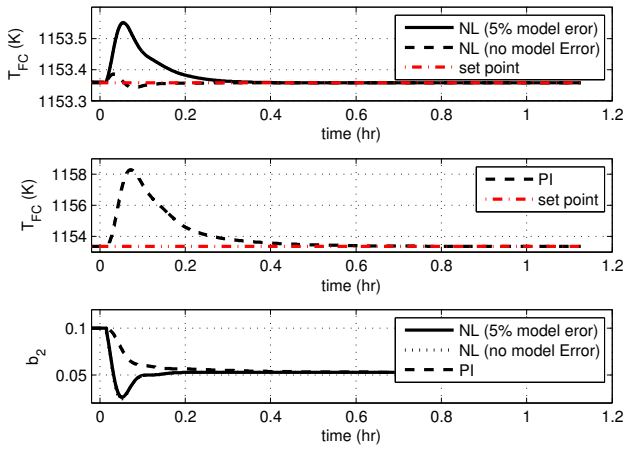

Fig. 3. Closed loop responses of fuel cell temperature and bypass ratio b_2

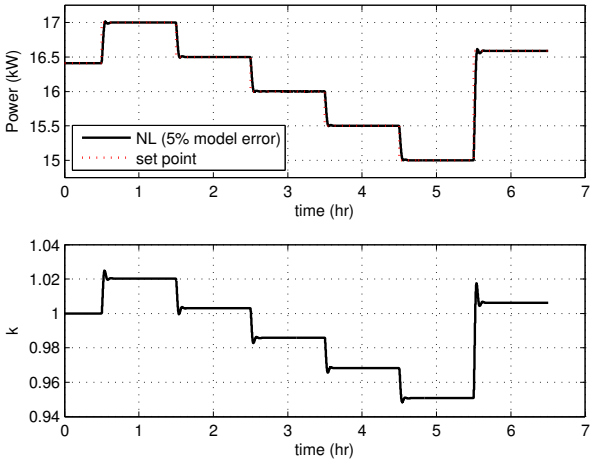

Fig. 4. Closed loop responses of power and DC/DC converter gain

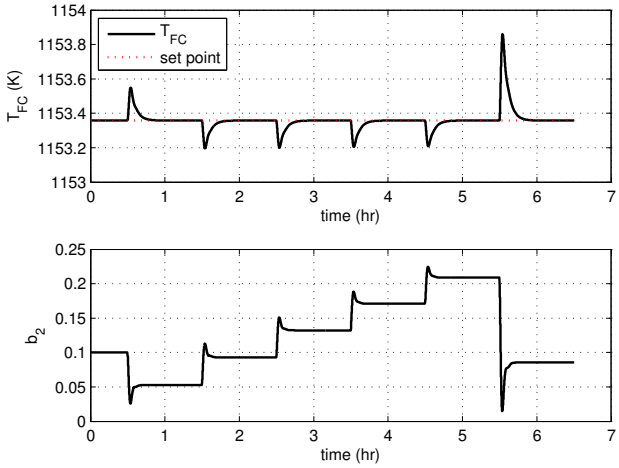

Fig. 5. Closed loop response of SOFC's temperature and bypass ratio b_2

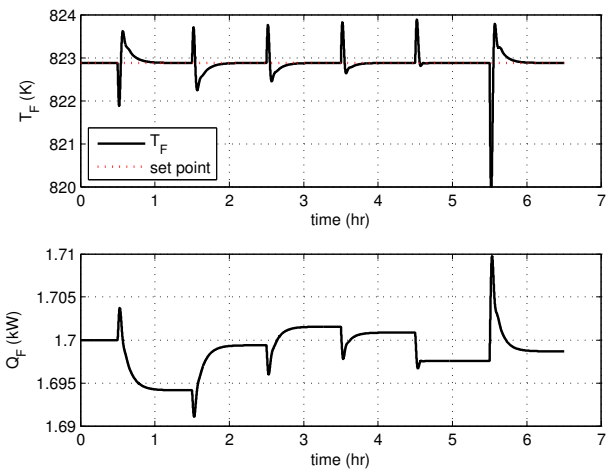

Fig. 6. Closed loop responses of furnace temperature and its heat duty

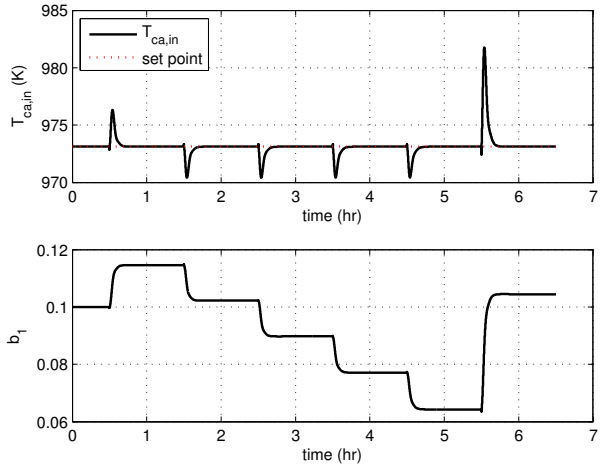

Fig. 7. Closed loop responses of air inlet temperature and bypass ratio b_2

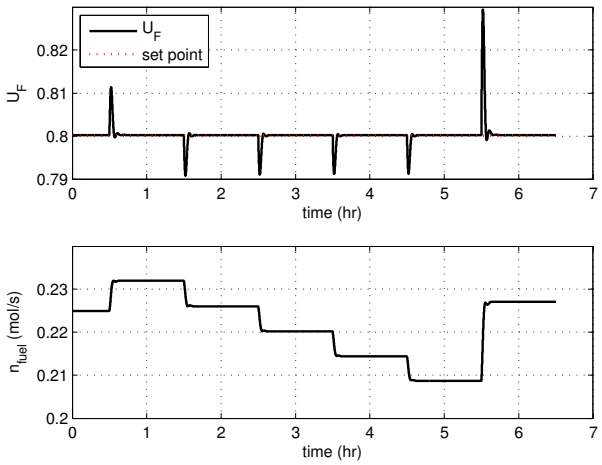

Fig. 8. Closed loop responses of fuel utilization and fuel inlet flow rate

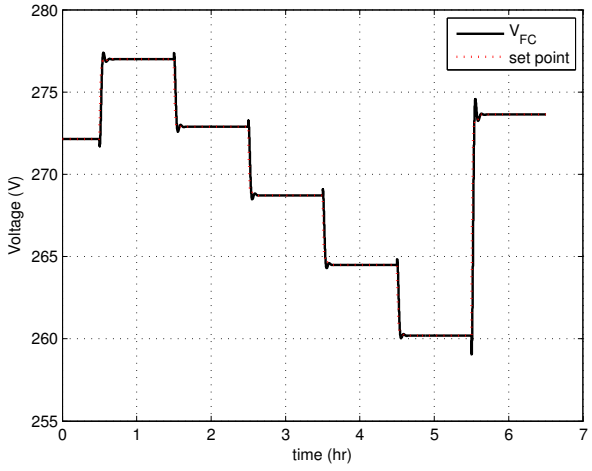

Fig. 9. Closed loop response of voltage

The nonlinear controller showed superior temperature regulation even in the presence of modeling errors. The behavior of the entire SOFC energy system was investigated under changes in the power demand. The proposed strategy yielded excellent performance in achieving the required power demand.

ACKNOWLEDGEMENTS

Partial financial support for this work from the Abu Dhabi - Minnesota Institute for Research Excellence, National Science Foundation Grant CBET-0756363 and the ACS-PRF is gratefully acknowledged. We are also thankful to Professor K. Nandakumar, for insightful discussions.

REFERENCES

[1] J. T. Pukrushpan, A. G. Stafanopoulou and H. Peng, *Control of Fuel Cell Power Systems: Principles, Modeling, Analysis and Feedback Design*; Springer, 2004.

[2] S. Varigonda and M. Kamat, "Control of Stationary and Transportation Fuel Cell Systems: Progress and Opportunities", *Comput. Chem. Eng.*, vol. 30, 2006, pp. 1735-1748.

[3] R.J. Kee, H. Zhu, A.M. Sukeshini and G.S. Jackson, "Solid oxide fuel cells: Operating principles, current challenges, and the role of syngas", *Combustion Science and Technology*, vol. 180, 2008, pp. 1207-1244.

[4] D. Bhattacharyya and R. Rengaswamy, "A review of solid oxide fuel cell (SOFC) dynamic models", *Ind. Eng. Chem. Res*, vol. 48, 2009, pp. 6068-6086.

[5] M. Bavarian, M. Soroush, I.G. Kevrekidis, and J.B. Benziger, "Mathematical Modeling, Steady-State and Dynamic Behavior, and Control of Fuel Cells: A Review",*Ind. Eng. Chem. Res*, vol. 49, 2010, pp. 7922-7950.

[6] H. Xi, J. Sun and V. Tsourapas, "A control oriented low order dynamic model for planar SOFC using minimum Gibbs free energy method", *Journal of Power Sources*, vol. 165, 2007, pp. 253-266.

[7] AKM M. Murshed, B. Huang and K. Nandakumar, "Control Relevant Modeling of Planer Solid Oxide Fuel Cell System", *J. Power Sources*, vol. 163, 2007, pp. 830-845.

[8] R. J. Braun, "Optimal Design and Operation of Solid Oxide Fuel Cell Systems for Small-scale Stationary Applications", *Ph. D. Thesis*, University of Wisconsin-Madison, 2002.

[9] A. M. Al-Qattan and D. J. Chmielewski, "Distributed Feed Design for SOFCs with Internal Reforming", *J. Electrochem. Soc.*, vol. 151, 2004, pp. A1891-A1898.

[10] R. Kandepu, L. Imsland, B. A. Foss, C. Stiller, B. Thorud and O. Bolland, "Modeling and Control of a SOFC-GT-based Autonomous Power System", *Energy*, vol. 32, 2007, 406-417.

[11] F. Mueller, R. Gaynor, A.E. Auld, J. Brouwer, F. Jabbari and G.S. Samuelsen, "Synergistic integration of a gas turbine and solid oxide fuel cell for improved transient capability" *J. Power Sources*, vol. 176, 2008, pp. 229-239.

[12] S-R, Oh. and J. Sun, "Optimization and load following characteristics of 5kW-Class tubular solid oxide fuel cell/gas turbine hybrid systems" *Proceedings in 2010 American Control Conference*, 2010, pp.417-422.

[13] F. Mueller, F. Jabbari, R. Gaynor, and J. Brouwer, "Novel solid oxide fuel cell system controller for rapid load following" *J. Power Sources*, vol. 172, 2007, pp. 308-323.

[14] X. Li, *Principles of Fuel Cells*; Taylor and Francis, 2006.

[15] H. Li, S. Varigonda, B. Jing, "Dynamic Modeling of a Solid Oxide Fuel Cell System for Control Design" *Proceedings in 2010 American Control Conference*, 2010, pp.423-428.

[16] J. Xu and G. F. Froment, "Methane Steam Reforming, Methanation and Water-Gas Shift: I. Intrinsic Kinetics", *AIChE J.*, vol. 35, 1989, pp. 88-96.

[17] S. Ahmed, and D. J. Chmielewski, "Load Characteristics and Control of a Hybrid Fuel Cell Battery Vehicle" *Proceedings in 2009 American Control Conference*, 2009, pp.2654-2659.

[18] P. Daoutidis, and C. Kravaris, "Dynamic output feedback control of minimum-phase multivariable nonlinear processes" *J. Chem. Eng. Sci.*, vol. 49, 1994, pp. 433-447

[19] F. Zenith, and S. Skogestad, "Control of fuel cell power output" *Journal of Process Control*, vol. 17, 2007, pp. 333-347